Available online at www.sciencedirect.com
SCIENCE DIRECT®
Surface Science 543 (2003) 118–130
SURFACE SCIENCE
www.elsevier.com/locate/susc

A theoretical study of surface-structural sensitivity of the reverse water-gas shift reaction over Cu(*hkl*) surfaces

Gui-Chang Wang [a,*], Ling Jiang [a], Xian-Yong Pang [b], Zun-Sheng Cai [a], Yin-Ming Pan [a], Xue-Zhuang Zhao [a], Yoshitada Morikawa [c], Junji Nakamura [d]

[a] *Department of Chemistry, Nankai University, Weijin Road 94, Tianjin 300071, PR China*
[b] *State Key Laboratory of C1 Chemistry & Technology, Taiyuan University of Technology, Taiyuan 030024, PR China*
[c] *Research Institute for Computational Sciences (RICS), and Research Consortium for Synthetic Nano-Function Materials Project (SNAF), National Institute of Advanced Industrial Science and Technology (AIST), Tsukuba Central 2, 1-1-1 Umezono, Tsukuba, Ibaraki 305-8568, Japan*
[d] *Institute of Materials Science, University of Tsukuba, Tsukuba, Ibaraki 305-8573, Japan*

Received 14 March 2003; accepted for publication 20 June 2003

Abstract

The surface-structural sensitivity of the reverse water-gas shift (RWGS) reaction ($CO_2 + H_2 \rightarrow CO + H_2O$) over the Cu(1 1 1), Cu(1 0 0), and Cu(1 1 0) surfaces has been studied by first-principle density functional calculations together with the UBI-QEP approach. Cluster models of the surface have been employed to simulate the adsorption of CO_2, H_2, H, O, OH, CO, and H_2O on the Cu(*hkl*) surfaces at low coverage. This sensitivity is determined by the difference in the activation barriers. It can be noticed that the most likely rate-determining step in RWGS reaction is the CO_2 dissociative adsorption, namely $CO_{2,g} \rightarrow CO_s + O_s$. The trend in the calculated activation barriers for the reaction of CO_2 dissociative adsorption follows the order of Cu(1 1 0) < Cu(1 0 0) < Cu(1 1 1), suggesting that the most efficient crystal surface for catalyzing RWGS reaction by copper is Cu(1 1 0), and the more densely packed Cu(1 1 1) surface is the least active among the Cu(*hkl*) surfaces studied here. As expected, the activation barriers for the recombinative reactions over Cu(*hkl*) are in the order of Cu(1 1 0) > Cu(1 0 0) > Cu(1 1 1), just opposite to the dissociative reactions. The interesting thing is that there is a good correlation between the adsorption bond length and the adsorption energy: The preferred adsorption site is the one with the shortest adsorption bond length. The present calculations are in good agreement with experimental observations.

Keywords: Surface structure, morphology, roughness, and topography; Water; Hydrogen molecule; Carbon monoxide; Carbon dioxide; Copper; Density functional calculations; Surface chemical reaction

1. Introduction

The catalytic water-gas shift (WGS) reaction ($CO + H_2O \rightarrow CO_2 + H_2$) is frequently applied in the chemical process industry; it also takes part in many proposed future technologies for energy

* Corresponding author. Tel.: +86-22-23507956/23504854; fax: +86-22-23502458.
E-mail address: wangguichang@nankai.edu.cn (G.-C. Wang).

0039-6028/$ - see front matter © 2003 Elsevier B.V. All rights reserved.
doi:10.1016/S0039-6028(03)00876-8

conversion (e.g. coal conversion to liquid fuels) [1]. For example, the steam reforming of hydrocarbons ($C_nH_m + nH_2O \rightarrow nCO + (n + m/2)H_2$) and the WGS reaction take place simultaneously. On the other hand, the reverse water-gas shift (RWGS) reaction ($CO_2 + H_2 \rightarrow CO + H_2O$), the reaction of carbon dioxide and hydrogen to produce carbon monoxide and water, is also a reaction of considerable industrial importance. The RWGS reaction technology is recently suggested in industries producing valuable CO from cheap CO_2 using hydrogen produced as a by-product. By the way, the hydrogenation of CO_2 usually reaches the production of CH_4 with transition metal catalysts at atmospheric pressure [2–5].

Both metal and metal oxides are common catalysts for the WGS reaction. The so-called "low-temperature" Cu/ZnO catalyst is widely used to catalyze this reaction. To study RWGS reaction, we borrow the same catalyst from WGS reaction for the moment. Indeed, the WGS and RWGS reactions have been studied over both high-surface-area catalysts containing Cu and ZnO [6–12] and model catalysts based on Cu single crystals, which have very well-controlled surface cleanliness and geometric structure [13–17]. Generally, two mechanisms (i.e. a formate mechanism and a "surface redox" mechanism) may be used to elucidate the WGS reaction on copper surface. According to the former, surface hydroxyls (OH_s) produced from dissociatively adsorbed H_2O combine with adsorbed CO (CO_s) to produce a surface formate intermediate ($HCOO_s$), which then decomposes to $1/2H_2$ and CO_2 [6–9]. While in the "surface redox" mechanism [6–12], H_2O surface-redox-dissociatively adsorbs to produce oxygen adatoms (O_s) and H_2, followed by the well-known reaction of CO with O_s to produce CO_2 (Ref. [9] and references therein). Very recently, the micro-kinetics of the WGS reaction has been investigated by Fishtik and Datta [19] utilizing the conventional transition state theory along with the unity bond index-quadratic exponential potential (UBI-QEP) method, indicating that the formate and associative mechanisms are dominant at lower temperatures while the redox mechanism is dominant at higher temperatures. Interestingly, the rate-determining step in both mechanisms is the same, i.e. the dissociative adsorption of water.

On the other hand, for the RWGS reaction the study of interaction of CO_2 with a clean Cu(1 1 0) surface supports a catalytic redox mechanism whereby the rate-determining step is the dissociative adsorption of CO_2, followed by consumption of the resulting O_s by reaction with $H_{2,g}$ [15]. This has also been confirmed by Ernst et al. [16] from the steady-state kinetic measurements and the analysis of RWGS reaction rate.

Real materials used in application normally expose a number of different crystallographic faces. The sensitivity of surface reactions to the crystallographic orientation of the surface is an interesting aspect to understand the catalysts. Some investigations [16–18] show that the RWGS reaction over the silica-supported copper catalysts is surface-structural sensitive. However, no systematic and detailed analysis on the energetic behavior of RWGS reaction on the Cu(*hkl*) surfaces can be found in the literature to our knowledge.

A property related to the surface-structural sensitivity is the adsorption energy of an adsorbate on different single crystal surfaces. In our previous reports [20,21] the interaction of C, H, O, and S atoms with the Cu(1 1 1) surface has been systematically studied from first-principle density functional calculations and the results agree well with the experiments. In this paper, the interaction of adsorbed species (i.e. CO_2, H_2, H, O, OH, CO, and H_2O) with the Cu(1 1 1), Cu(1 0 0) and Cu(1 1 0) surfaces will be studied by density functional techniques to elucidate the equilibrium geometry and the binding characteristics. Because it is difficult to locate the transition states of the RWGS reaction on these surfaces, we focus mainly on an evaluation of dissociation or recombination energies, and then follow Shustorovich's approach [22–24] to determine the activation barriers of elementary reactions. Shustorovich [22,23] has developed the so-called bond-order conservation Morse-potential (BOC-MP) method to treat the dissociations of adsorbates on metal surfaces, and the analytical BOC-MP formula relates the activation energy to the dissociation or recombination energies and the adsorption energies of an adsorate and its dissociative fragments. Recently, Shustorovich and Sellers [24] have made a considerable revision to the BOC-MP method and

renamed as the unity-quadratic exponential potential (UBI-QEP) method. However, the analytical expression for estimating activation barriers remains unchanged. The UBI-QEP method demonstrated in every case [21–26] can provide an efficient and fast way to evaluate the activation barriers. We will limit our description of the method to a brief summary of the equations required for the present study (see Appendix A). The reader could refer to the work of Shustorovich and Sellers [23,24] for an in depth discussion on the UBI-QEP approach.

2. Cluster models and computational methods

The cluster model has been used frequently to investigate the chemical interaction of the adsorbates with the metal surfaces. Many papers have been published [20,21,26–30], in which cluster models have provided accurate descriptions of adsorbate geometry, vibrations and energetics. The development of modern surface science provided the opportunity to investigate the interaction between catalysts and molecules or atoms in the atomic scale. However, computations of molecules containing transition metal atoms have proven to be more difficult than those for first- and second-row atoms [30]. Recent advances in methodology based on the technologies of pseudopotential and plane-wave basis sets and the high-speed computers have now made it possible to obtain quantitative information on the surface phenomena.

In this work, cluster models of the surface have been employed to simulate CO_2, H_2, H, O, OH, CO, and H_2O adsorbed on the Cu(1 1 1), Cu(1 0 0) and Cu(1 1 0) surfaces. The copper cluster models of Cu_{18}(15,3) (i.e. 15 atoms in the first and three atoms in the second layer), and Cu_{18}(12,6) (i.e. 12 atoms in the first, six atoms in the second layer) shown in Fig. 1 have been chosen to represent the Cu(1 1 1), Cu(1 0 0) and Cu(1 1 0) surfaces, respectively. The Cu(1 1 1), Cu(1 0 0) and Cu(1 1 0) surfaces are constructed using the bulk lattice constants of 3.615 Å [31]. Our recent investigation of the interaction of CO_2 with the Cu(*hkl*) surfaces (unpublished results) demonstrates that the Cu_{18}(15,3) and Cu_{18}(12,6) cluster models can provide accurate descriptions of the interaction between well-defined single crystal copper surfaces and small molecules or atoms such as CO_2, H_2, O. Generally, there are four different adsorption sites on the Cu(1 1 1) crystal surface: the atop site which resides above a surface atom, two 3-fold hollow sites which correspond to the "fcc site" and the "hcp site" (the hcp site resides above an atom of the second substrate layer; the fcc site does not), and the "bridge" site which lies halfway between the fcc and hcp sites. Similarly, the 4-fold hollow site, short bridge (SB) or long bridge (LB) site, and the top site could be found in the Cu(1 0 0) and Cu(1 1 0) surfaces. These sites are schematically illustrated in previous study [21]. In the present calculations, the geometry of metal cluster was kept unchanged while the geometry of adsorbates above the surface was fully optimized, which is based on the fact that there is indeed very little modification of the metal surface by adsorbed species at low coverage [32,33].

The interaction of CO_2, H_2, H, O, OH, CO, and H_2O with the different adsorption sites on Cu(1 1 1), Cu(1 0 0) and Cu(1 1 0) surfaces has been studied by first-principle density functional calculations that use the hybrid B3LYP

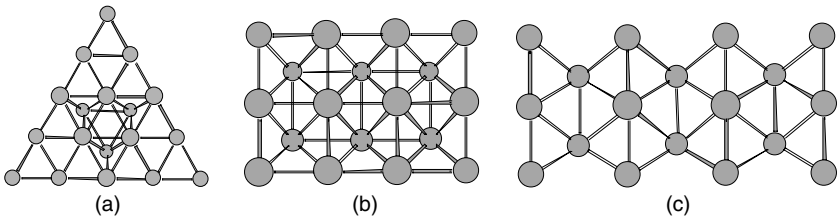

Fig. 1. The Cu_{18}(15,3) and Cu_{18}(12,6) cluster models represent the Cu(1 1 1), Cu(1 0 0), and Cu(1 1 0) surfaces, respectively. (a) Cu_{18}(15,3)–(1 1 1), (b) Cu_{18}(12,6)–(1 0 0), and (c) Cu_{18}(12,6)–(1 1 0).

exchange-correction functional [34,35] as implemented in Gaussian94 program package [36]. For Cu atoms, the relativistic effective core potentials (ECP) reported by Hay and Wadt [37] have been used to describe the 1s–2p core while the electrons arising for the 3s, 3p, 3d, 4s, 4p shells are treated explicitly. It is customary to refer to these ECPs as LANL2. The standard double-ζ basis set, also reported by Hay and Wadt [37] and denoted as usual as LANL2DZ, is used to describe the electron density of the valence electrons of Cu. Based on analysis of BSSE in our recent study of the interaction of CO_2 with Cu(*hkl*) surfaces (unpublished results) and previous study [21], the electron densities of C, O, and H atoms are described with the standard 6-31G basis set.

Manifesting the high level of accuracy in calculations of atomic and molecular chemisorption energies on metal surfaces, the UBI-QEP method demonstrated in every case [21–26] can provide a useful way to evaluate the activation barriers. The highest adsorption energies of CO_2, H_2, H, O, OH, HCOO, CO, and H_2O on Cu(*hkl*) from first-principle DFT calculations together with the dissociation energy of these molecules in the gas phase can be used to determine the activation barriers of forward reactions (E_f) and reversed reactions (ΔE_r) and enthalpy changes (ΔH) for reverse water-gas Shift reaction on the Cu(1 1 1), Cu(1 0 0), and Cu(1 1 0) surfaces. The appendix provides a brief summary of the equations required for the present study.

One should further comment on the UBI-QEP analysis of the surface reactivity. Remember that the reaction rate constants k of an elementary process is described in the Arrhenius form as [6]

$$k = A\exp(-E^*/RT)$$

where A is a pre-exponential factor and E^* is an activation barrier. Because of their exponential effect, the values of E^* are usually critical, however, the values of A should be close in order to make a decisive comparison between two reactions based solely on the values of E^*. This condition is most likely to be met for a given reaction on a surface with given orientation, say fcc(1 1 1), though of two different metals, say Fe(1 1 1) and Ni(1 1 1). However, the next best case will be for two reactions of the same reaction order on a given surface.

3. Results and discussion

Tables 1–3 list the adsorption energies and structural parameters of CO_2, H_2, H, O, OH, CO, and H_2O adsorbed onto the Cu(1 1 1), Cu(1 0 0) and Cu(1 1 0) surfaces, together with available experimental data. The adsorption energy (E) is calculated according to the formula:

Table 1
Adsorption energies (E) and structural parameters for the reactants (CO_2 and H_2) adsorbed onto the Cu(1 1 1), Cu(1 0 0), and Cu(1 1 0) surfaces[a]

CO_2	R_{Cu-C}/Å	C–O distance/Å		O–C–O angle/°	E_{CO_2} (DFT)/eV	E_{CO_2} (exptl)/eV	Ref.
		Left O–C	Right C–O				
Cu(1 1 1)	3.353	1.187	1.189	179.98	0.20	0.19	[40]
Cu(1 0 0)	3.251	1.188	1.188	178.93	0.23	0.26–0.31	[42]
Cu(1 1 0)	3.102	1.192	1.182	179.98	0.33		
H_2	Site	R_{Cu-H}/Å	R_{H-H}/Å	Tilting angle/°	E_{H_2} (DFT)/eV	E_{H_2} (exptl)/eV	
Cu(1 1 1)	Top	2.376	0.746	1.00	0.21		
Cu(1 0 0)	Top	2.297	0.747	2.80	0.30		
Cu(1 1 0)	Hollow	3.121	0.745	3.81	0.18		
Cu(1 1 0)	LB	2.537	0.746	1.82	0.26		
Cu(1 1 0)	Top	2.195	0.749	0.17	0.36	0.35–0.52	[43]

[a] R_{Cu-C} or R_{Cu-H}, the distance from Cu atom to the nearest C or H atom.

Table 2
Adsorption energies (E) and structural parameters for intermediate fragments (H, O, and OH) adsorbed onto the Cu(1 1 1), Cu(1 0 0), and Cu(1 1 0) surfaces

H	R_{Cu-H}/Å	E_H (DFT)/eV	E_H (exptl)/eV	Ref.	
Cu(1 1 1)-hcp	1.793	2.01			
Cu(1 1 1)-fcc	1.776	2.19	2.43	[44]	
Cu(1 0 0)-hollow	1.720	2.38			
Cu(1 1 0)-hollow	2.273	1.77			
Cu(1 1 0)-SB	1.695	2.62			
O	R_{Cu-O}/Å	E_O (DFT)/eV	E_O (exptl)/eV		
Cu(1 1 1)-hcp	1.957	4.19			
Cu(1 1 1)-fcc	1.940	4.39	4.47	[46]	
Cu(1 0 0)-hollow	1.919	4.60			
Cu(1 1 0)-LB	1.826	4.76			
OH	R_{Cu-O}/Å	R_{O-H}/Å	Tilting angle/°	E_{OH} (DFT)/eV	E_{OH} (exptl)/eV
Cu(1 1 1)-hcp	2.025	0.959	2.70	2.62	
Cu(1 1 1)-fcc	1.995	0.963	1.00	2.70	
Cu(1 0 0)-bridge	1.930	0.969	0.18	2.40	
Cu(1 0 0)-hollow	1.916	0.975	1.02	2.86	
Cu(1 1 0)-hollow	1.901	0.986	0.20	2.96	
Cu(1 1 0)-LB	1.886	0.996	0.08	3.07	

Table 3
Adsorption energies (E) and structural parameters for the products (CO and H_2O) adsorbed onto the Cu(1 1 1), Cu(1 0 0), and Cu(1 1 0) surfaces

CO	R_{Cu-C}/Å	R_{C-O}/Å	Tilting angle/°	E_{CO} (DFT)/eV	E_{CO} (exptl)/eV		Ref.
Cu(1 1 1)	2.222	1.151	0.08	0.50	0.72		[51]
Cu(1 0 0)	2.126	1.156	1.12	0.72	0.80		[51]
Cu(1 1 0)	1.990	1.157	1.18	0.81	0.85		[51]
H_2O	R_{Cu-O}/Å	H–O distance/Å		H–O–H angle/°	E_{H_2O} (DFT)/eV	E_{H_2O} (exptl)/eV	
		Left H–O	Right O–H				
Cu(1 1 1)	2.162	0.974	0.976	111.15	0.61	0.40–0.70[a]	[54]
Cu(1 0 0)	2.078	0.980	0.976	112.76	0.81		
Cu(1 1 0)	2.003	0.993	0.973	111.01	1.00		

[a] The data were measured on an unspecified orientation metal surface.

$$E = E(\text{cluster}) + E(\text{adsorbate}) - E(\text{cluster} + \text{adsorbate}) \quad (1)$$

where E(cluster), E(adsorbate), and E(cluster + adsorbate) denote the calculated energy of a cluster without adsorbate, the free adsorbate, and a cluster with adsorbate, respectively. A positive value of E implies that the adsorption of adsorbate from gas-phase is thermodynamically favorable. From the calculated adsorption energies, the distances from Cu atom to the nearest C, H, or O atom, and the intramolecular bond lengths reported in Tables 1–3, it can be inferred that the relative strength of adsorption for adatom (i.e. H or O) or radical (i.e. OH) is stronger than that for molecule (i.e. CO_2, H_2, CO, or H_2O) on a given surface.

3.1. Adsorptions of the reactants (CO_2, H_2)

In general, a major objective in studying CO_2-surface interactions is investigating its activation

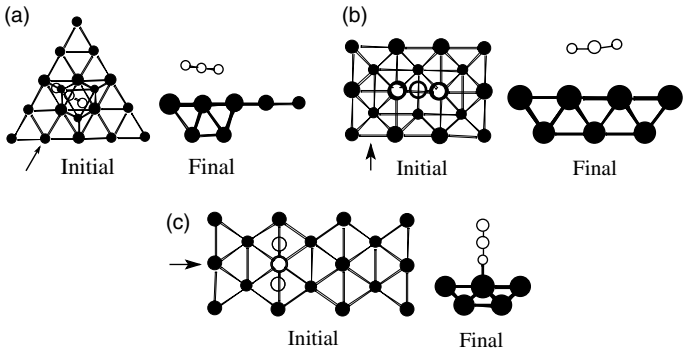

Fig. 2. Top views of the initial forms and side views of final optimized forms of CO_2 adsorbed onto: (a) Cu(1 1 1), (b) Cu(1 0 0), and (c) Cu(1 1 0) surfaces. (The directions of side views are as indicated by arrows in the initial forms.) In the view of final optimized form, the oxygen atom on the left of carbon atom is labeled as "Left O" in text and Table 1.

because of the implication of CO_2-activation in many chemical processes with the cheap C1 feedstock. Solymosi [38] and Freund and Rorbert [39] have provided comprehensive reviews for CO_2 interaction with clean and modified single crystal metal surfaces and real catalyst surfaces. Our representative results of top views of the initial forms and side views of final optimized forms of CO_2 adsorbed onto the Cu(1 1 1), Cu(1 0 0), and Cu(1 1 0) surfaces with the largest adsorption energy are shown in Fig. 2. These optimized results indicate that the final structure of adsorbed CO_2 is near linear and the preferred modes for the adsorption of CO_2 onto the Cu(1 1 1), Cu(1 0 0), and Cu(1 1 0) surfaces are the side-on adsorption at the cross-bridge site with an adsorption energy of 0.20 eV, the side-on adsorption at the short bridge site (0.23 eV), and the end-on adsorption on the on-top site with C–O bonds locating along the short bridge site (0.33 eV), respectively. In addition, the slightly elongated C–O bond length in $CO_{2,s}$ indicates the activation of CO_2. Therefore, the adsorption energies for the nonpolar CO_2 are small and in the order of Cu(1 1 0) > Cu(1 0 0) > Cu(1 1 1).

Carbon dioxide is thought to be adsorbed on polycrystalline Cu both in physisorbed form with the adsorption energy (E) of 0.19 eV [40] and in an anionic (CO_2^-) chemisorbed state ($E < 0.62$ eV) [41]. The interaction of carbon dioxide with Cu(1 0 0) surface has been investigated by TPD and the adsorption energy has been measured to be 0.26–0.31 eV in the coverage range 0.05–0.40 ML [42]. From Table 1 it is easy to find that the calculated results agree well with the experiments. Among other studies, the highest adsorption energy of CO_2, computed by Au and Chen [32] with the Slater DFT code on a $Cu_{14}(9,4,1)$ cluster which is taken as a cluster model of the Cu(1 0 0) surface, was 0.27 eV, which also is in good agreement with the experimental value 0.26–0.31 eV [42].

For the adsorption of H_2 on the Cu(*hkl*) surfaces, the adsorption energies involved are also small, with magnitudes less than 0.40 eV. This is to be expected as H_2 is a nonpolar molecule. The optimized molecular axis of $H_{2,s}$ is nearly normal to the surface. The H_2 adsorption at the top site of Cu(1 1 1), Cu(1 0 0), and Cu(1 1 0) is found to be energetically preferred with an adsorption energy of 0.21, 0.30, and 0.36 eV, respectively. The slightly elongated H–H distance from free H_2 molecule (0.741 Å) [31] demonstrates that the H–H bond in adsorbed H_2 molecule gains somewhat activation. This kind of weakly adsorbed behavior is consistent with the experimental observations [43].

3.2. Adsorptions of intermediate fragments (H, O, OH, HCOO)

Previous study of the atomic hydrogen adsorption on the Cu(1 1 1) surface [20] has shown that H prefers the high-coordination three hollow site. Thus, for Cu(1 1 1) the only geometries of H

adatom considered in the present work are on the fcc and hcp sites. The results are collected in Table 2, together with results on Cu(1 0 0) and Cu(1 1 0) surfaces and the available experiment data. It is easy to find from Table 2 that H atom can adsorb strongly on the Cu(*hkl*) surfaces. The calculated adsorption energy of H atom at the fcc site of Cu(1 1 1) (2.19 eV) is in accord with the experimental value 2.43 eV [44]. Interestingly, the final optimized site of H atom on Cu(1 1 0) is short-bridge (SB) site from the initial site of long-bridge (LB). The preference of SB site for hydrogen atomic adsorption on the Cu(1 1 0) surface is different from O atom whereas the most stable position for oxygen is the LB site [21,45].

Based on the systematic investigation of the equilibrium geometry and the binding characteristics of atomic oxygen on the Cu(1 1 1), Cu(1 0 0) and Cu(1 1 0) surfaces [21], only four preferred sites of atomic oxygen on Cu(*hkl*) have been optimized in this work. The calculated adsorption energies (listed in Table 2) are 4.19–4.76 eV, in good agreement with the experiments [45,46] and the previous B3LYP hybride calculations [21].

The adsorption of small molecular radicals at metal surfaces is of considerable experimental as well as theoretical interest since they are present and can occur as the reaction intermediates in heterogeneous catalytic processes. For example, OH is found as a component in the catalytically activated hydrogen–oxygen reaction or in the water-gas shift reactions. For the adsorption of OH on Cu(*hkl*), the present optimized results show that OH stabilizes with its molecular axis nearly normal to the copper surface and the oxygen pointing towards the metal. OH prefers the fcc hollow, 4-fold hollow site, and long-bridge site on the Cu(1 1 1), Cu(1 0 0), and Cu(1 1 0) surfaces with an adsorption energy of 2.70, 2.76, 3.07 eV, respectively. As a comparison, among other studies, the fcc site of Cu(1 1 1) is found to be energetically preferred with an OH/Cu binding energy of 3.10 eV at the configuration interaction (CI) level [27], but OH_s is also negative charged in the presence of surface with the formation of ionic surface bond.

In the case of HCOO, Hu and Boyd [29] have investigated the adsorption behavior of formate on the Cu(*hkl*) surfaces using the DFT method, and found that the calculated geometries and vibrational frequencies were in good agreement with experimental data. According to the adsorption energies, however, the comparison between DFT method and experiments could not be found in their work. For the moment, the adsorption energies HCOO (Table 4) are calculated using the UBI-QEP method (see Appendix A) based on the reliable adsorption energies for O atom from the present DFT calculations (Table 2). Indeed, we plan to investigate the formate decomposition pathway in future studies.

Table 4
The adsorption energies of the adsorbates on Cu(*hkl*) and the dissociation energy of molecules in the gas phase (units: eV)

Adsorbate	Cu(1 1 1)	Cu(1 0 0)	Cu(1 1 0)	D_{AB}[a]
CO_2	0.20	0.23	0.33	16.65 (5.52[b])
H_2	0.21	0.30	0.36	4.52
H	2.19	2.38	2.62	
O	4.39	4.60	4.76	
OH	2.70	2.86	3.07	4.43
CO	0.50	0.72	0.81	11.16
H_2O	0.61	0.81	1.00	9.54
HCOO	0.34	1.13	1.81	16.65

[a] The dissociation energies (D_{AB}) are taken from Ref. [23].
[b] The value in parentheses represents the CO–O bond strength taken from Ref. [29].

3.3. Adsorptions of the products (CO, H_2O)

There are many experimental and theoretical studies of the interaction between CO and transition metal surfaces because of the potential use of Fischer–Tropsch chemistry in the production of hydrocarbons and synthetic alcohol fuels. A good review can be found in Ref. [47]. A few of the most important points will be cited with more recent results. It can be concluded from previous studies [47–50] that at low coverage CO prefers the top site on the copper surface with the carbon end down. From Table 3, the CO molecule is found to be slightly tilted with angle of 0.08–1.18, suggesting that the molecular axis of CO is nearly normal to the surface. One can see that the calculated adsorption energies on the Cu(*hkl*) surfaces (0.50–0.81 eV) are quite close to the experimental data (0.72–0.85 eV) [51]. In addition, the slightly elongated C–O distances in adsorbed CO further

confirm the weakly adsorbed behavior of CO on the copper surfaces. This again agrees well with various experimental evidences [47–49].

For H_2O adsorption, the side views of the initial forms and top views of final optimized forms of water adsorbed onto the Cu(1 1 1), Cu(1 0 0), and Cu(1 1 0) surfaces are schematically shown in Fig. 3. The top site on Cu(*hkl*) is found to be energetically most favorable. Water bonds through the oxygen atom to the surface. Similarly, calculations with metal clusters by Müller and Harris [52] and Ribarsky et al. [53] point to an on-top tilted geometry as the most favorable. Finally, the calculated adsorption energies of H_2O on the Cu(1 1 1), Cu(1 0 0), and Cu(1 1 0) surfaces are 0.61, 0.81, and 1.00 eV respectively, which may be with a bigger deviation than the other adsorbed species from the available experimental data (0.40–0.70 eV) [54,55]. However, because of the uncertainty on surface orientation in Ref. [54], this deviation is not for sure yet.

From Tables 1–3, one may reach a conclusion that the adsorption energies for a given adsorbate are in the order of Cu(1 1 0) > Cu(1 0 0) > Cu(1 1 1) at low coverage, and consistent with the order in the distances from Cu atom to the nearest C, H, or O atom and the intramolecular bond lengths, suggesting that the relative strength of adsorption for the adsorbates on Cu(*hkl*) may be characterized by several indexes.

3.4. Energetics for the RWGS reaction over Cu(hkl) surfaces

In this section, the energetics of the RWGS reaction on the Cu(*hkl*) surfaces will be discussed in terms of the elementary reaction steps in the surface mechanism. Considering that the reaction pathway of molecule dissociation maybe involve surface dissociation or dissociative adsorption, the possible elementary reactions of the RWGS reaction are summarized as

$$CO_{2,g} \rightarrow CO_{2,s} \quad [R1]$$

$$CO_{2,s} \rightarrow CO_s + O_s \quad [R2]$$

$$CO_{2,g} \rightarrow CO_s + O_s \quad [R3]$$

$$H_{2,g} \rightarrow H_{2,s} \quad [R4]$$

$$H_{2,s} \rightarrow 2H_s \quad [R5]$$

$$H_{2,g} \rightarrow 2H_s \quad [R6]$$

$$H_s + O_s \rightarrow OH_s \quad [R7]$$

$$H_s + OH_s \rightarrow H_2O_s \quad [R8]$$

$$CO_{2,s} + H_s \rightarrow HCOO_s \quad [R9]$$

$$HCOO_s \rightarrow CO_s + OH_s \quad [R10]$$

$$CO_{2,s} + H_s \rightarrow CO_s + OH_s \quad [R11]$$

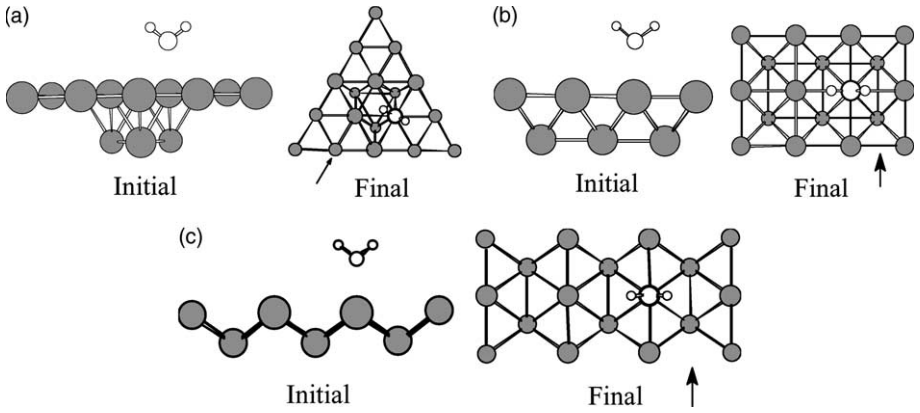

Fig. 3. Side views of the initial forms and top views of final optimized forms of H_2O adsorbed onto: (a) Cu(1 1 1), (b) Cu(1 0 0), and (c) Cu(1 1 0) surfaces. (The directions of side views are as indicated by arrows in the final forms.) In the view of final optimized form, the hydrogen atom on the left of oxygen atom is labeled as "Left H" in text and Table 3.

$CO_s \rightarrow CO_g$ [R12]

$H_2O_s \rightarrow H_2O_g$ [R13]

Based on the highest adsorption energies of CO_2, H_2, H, O, OH, HCOO, CO, and H_2O on Cu(*hkl*) from first-principle DFT calculations together with the dissociation energy of these molecules in the gas phase (Table 4), the UBI-QEP formula is employed and we report the calculated activation barriers and enthalpy changes in Table 5, respectively. In addition, the activation barriers of forward reactions (ΔE_f) for RWGS reaction on the Cu(1 1 1), Cu(1 0 0), and Cu(1 1 0) surfaces are comparatively shown in Fig. 4. The rather negative values of ΔE indicate that these reactions on the Cu(*hkl*) surfaces are very favorable.

From Table 4, one may observe that the adsorption energies of molecules (i.e. CO_2, CO, H_2, H_2O) are small. So, if the reaction could find a pathway of dissociative adsorption to avoid the difficulty of molecular adsorption, it will be the dominant pathway. In the RWGS reaction mechanism, we find that R3 is the optimal pathway for CO_2 dissociation. For R3 ($CO_{2,g} \rightarrow CO_s + O_s$), the estimated activation barriers on Cu(1 0 0) and Cu(1 1 0) are 0.82 and 0.64 eV respectively, which are in good agreement with the experimental data, i.e. 0.96 ± 0.05 eV [42] and 0.70 eV [15], respectively.

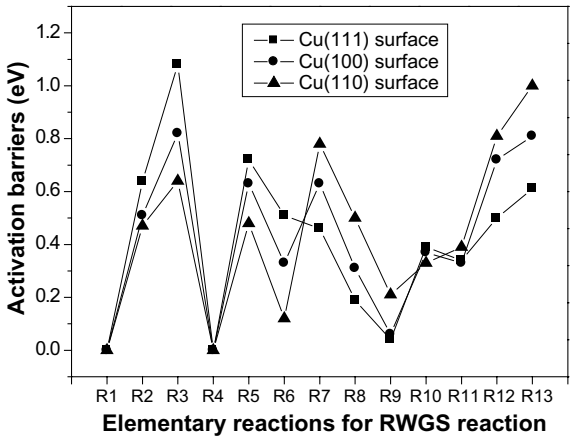

Fig. 4. Schematic illustration of calculated activation barriers (E^*) of elementary reactions for reverse water-gas shift reaction on the Cu(1 1 1), Cu(1 0 0), and Cu(1 1 0) surfaces.

For the H_2 dissociation (i.e. $H_{2,s} \rightarrow 2H_s$) on the Cu(1 1 0) surface, the calculated activation barrier of 0.48 eV is consistent with the experiments (0.60 ± 0.06 eV) [53]. Meanwhile, the trend in activation barriers for the reaction R5 or R6 over Cu(*hkl*) also follows the order of Cu(1 1 0) < Cu(1 0 0) < Cu(1 1 1), indicating that the Cu(1 1 0) is more reactive with respect to H_2 and CO_2 dissociative adsorption. From the combinative energies for the reaction R7 and R8 listed in Table 5, one can see that the recombinations of H_s and O_s

Table 5
Activation barriers of forward reactions (ΔE_f) and reversed reactions (ΔE_r) and enthalpy changes (ΔH) for reverse water-gas shift reaction on the Cu(1 1 1), Cu(1 0 0), and Cu(1 1 0) surfaces (units: eV)

Reactions	Cu(1 1 1)			Cu(1 0 0)			Cu(1 1 0)		
	ΔE_f	ΔE_r	ΔH	ΔE_f	ΔE_r	ΔH	ΔE_f	ΔE_r	ΔH
R1	0.00	0.20	−0.20	0.00	0.23	−0.23	0.00	0.33	−0.33
R2	0.64	0.00	0.80	0.51	0.11	0.40	0.47	0.22	0.25
R3	1.08	0.45	0.63	0.82	0.62	0.20	0.64	0.69	−0.05
R4	0.00	0.21	−0.21	0.00	0.30	−0.30	0.00	0.36	−0.36
R5	0.72	0.37	0.35	0.63	0.57	0.06	0.48	0.84	−0.36
R6	0.51	0.58	−0.07	0.33	0.87	−0.54	0.12	1.20	−1.08
R7	0.46	1.01	−0.55	0.63	0.94	−0.31	0.78	0.78	−0.12
R8	0.19	1.02	−0.83	0.31	0.99	−0.68	0.50	0.92	−0.42
R9	0.04	0.14	−0.10	0.06	0.14	−0.08	0.21	0.10	0.11
R10	0.39	0.04	0.35	0.37	0.20	0.17	0.33	0.29	0.02
R11	0.34	0.09	0.25	0.33	0.24	0.09	0.39	0.26	0.13
R12	0.50	0.00	0.50	0.72	0.00	0.72	0.81	0.00	0.81
R13	0.61	0.00	0.61	0.81	0.00	0.81	1.00	0.00	1.00

to OH_s, and consequently with H_s to H_2O_s on the Cu(*hkl*) surfaces are exothermic. The interesting thing is that the activation barrier for recombinative reaction (i.e. R2, R3, R5, R6, R7, or R8) is in the order of Cu(1 1 0) > Cu(1 0 0) > Cu(1 1 1), suggesting that the surface reactivity for these recombinative reactions are as expected just opposite to the dissociative reactions here (shown in Fig. 4) and the water dissociation ($H_2O_s \rightarrow OH_s + H_s$) from previous study [21]. This phenomenon reflects that the difference between a Lewis acid (i.e. CO_2) and a Lewis base (i.e. H_2O) is not noticeable. Because the dissociative reaction requires a higher energy to cleave bond, it has to have a closer interaction with the metal surface structure. So, the bigger the coordinately unsaturated degree of surface metal atom is, the easier is the bond cleavage. Of course, further experimental supports for these observations are needed.

As mentioned above, the deviation in the calculated adsorption energies for water on Cu(*hkl*) may be out of the error range for other adsorbed species (i.e. CO_2, CO, O, H, and OH), indicating that the surface cluster models and/or basis set used here may be less fit for H_2O than for other adsorbed species. This observation implies that one should be further aware of the surface cluster approximation and basis set effect in the modeling study. Since the adsorption energies of CO_2, H_2, H_2O, and CO are all rather small, it has been demonstrated that the coverage of these molecules is undoubtedly below a few percent of monolayer at 673 K during the RWGS reaction [14]. So, one could exclude the possibility that the desorption processes of CO and H_2O would dominate the rate of RWGS reaction.

The apparent activation barrier of formate synthesis from CO_2 and H_2 is ca. 0.58 eV over copper surfaces [57]. Taylor et al. [58] reported that activation barrier of $CO_{2,s} + H_s \rightarrow HCOO_s$ is 0.91 eV over Cu(1 0 0) surface. No matter how, the present calculated activation barriers (0.04–0.21 eV) of R9 are underestimated, due to the fact that the difference in dissociation energies between reactants and products of R9 is assumed to zero, namely $D = 0$, in the calculation [23]. Generally, there are two pathways in the decomposition of surface formate species, namely, dehydrogenation that leads to the production of CO_2 and H_2, and dehydration resulting in the production of CO and H_2O. It has been reported formate decomposes only via dehydrogenation on Cu(1 1 0) [59–61], Cu(1 0 0) [62,63], Cu(1 1 1) [64], and Pt(1 1 1) [65], suggesting that the activation barriers of R10 (i.e. $HCOO_s \rightarrow CO_s + OH_s$) is very high. Thus, the elementary step of CO_2 dissociation is necessary for RWGS reaction.

From the activation barriers (ΔE) listed in Table 5, it seems that one of the reactions of R3 and R7 may possible be the rate-determining step in RWGS reaction excluding the desorption of products. However, the activation barrier of the subsequent reaction (i.e. R8) is significant lower than that of R7. So both O_s and OH_s could be rapidly consumed through R7 and R8. Thus, the activation barrier (ΔE) of R3 plays a more important role in the RWGS reaction, and it could be identified as the rate-determining step in RWGS reaction, which is consistent with the experimental observations [12,15–19]. This conclusion was also supported by the fact that the dissociative adsorption probability for H_2 ($\sim 10^{-5}$ at 673 K [56]) is several orders of magnitude larger than that for CO_2 ($\sim 10^{-8}$ at 673 K [15]) at least on clean Cu(1 1 0). And this difference would normally result in a switch in the rate-determining step from R3 to R7 at H_2/CO_2 ratios well below unity. Based on the above-analyzed trends for the CO_2 molecular surface dissociation energies in R2 and activation barriers in R3, the catalytic activity for the RWGS reaction is in the order of Cu(1 1 0) > Cu(1 0 0) > Cu(1 1 1), which is in line with the experiments [15–18]. This is probably due to the fact that the (1 1 0) plane is such a properly open surface that its surface Cu atoms are much more coordinately unsaturated and hence more favorable in chemisorptive bonding. It was previous [21] shown that the WGS reaction determined by the dissociative adsorption of H_2O on Cu(*hkl*) was also surface-structural sensitive with the activation barrier in the order of Cu(1 1 0) (0.95 eV) < Cu(1 0 0) (1.03 eV) < Cu(1 1 1) (1.18 eV), which is consistent with the experimental observations [14,16]. Furthermore, the RWGS reaction may be more surface-structurally sensitive (the activation barrier difference for the CO_2 dissociation between

Cu(1 1 1) and Cu(1 1 0) is 0.44 eV (in Table 5) than the WGS reaction (0.10 eV in Table 5, 0.23 eV in Ref. [21]).

4. Conclusions

In the present work, the first-principle density functional calculations together with the UBI-QEP method have been performed to investigate the surface-structural sensitivity of the RWGS reaction on the Cu(*hkl*) surfaces. Cluster models of the surface have been employed to simulate CO_2, H_2, H, O, OH, CO, and H_2O adsorbed on the Cu(1 1 1), Cu(1 0 0) and Cu(1 1 0) surfaces at low coverage. Optimized results show that the adsorption energies for CO_2 and H_2 molecules are the smallest resulting in the weakest adsorption, while H, O, and OH can adsorb rather strongly on the Cu(*hkl*) surfaces. The adsorption for CO and H_2O, which are the products in the RWGS reaction, is stronger than that for CO_2 and H_2, which are the reactants in the reaction.

Based on the results from DFT calculations, the activation barriers of elementary reactions for the RWGS reaction on the Cu(1 1 1), Cu(1 0 0), and Cu(1 1 0) surfaces have been evaluated using the analytic UBI-QEP formula. The activation barrier is shown to be an important factor distinguishing the pathway for the RWGS reaction on different single crystal surfaces. It can be observed that the rate-determining step in the RWGS reaction is the CO_2 dissociative adsorption, namely $CO_{2,g} \rightarrow CO_s + O_s$. The trend in calculated activation barriers implies that the RWGS reaction rate might follow the order of Cu(1 1 0) > Cu(1 0 0) > Cu(1 1 1). We also note that the surface reactivity for the $H_s + OH_s \rightarrow H_2O_s$ reaction is in the order of Cu(1 1 0) < Cu(1 0 0) < Cu(1 1 1), just opposite to the dissociative reaction. The surface-structural sensitivity of the RWGS reaction over Cu(*hkl*) surfaces is in accord with the experimentally observed tendency. Frankly, it should be pointed out that the combined strategy of DFT calculations with UBI-QEP approach is somewhat simple. We plan to deconvolve rigorous and detailed DFT calculations of the decomposition pathway of molecules (i.e. HCOO, H_2O, CO_2, etc.) on transition metal surfaces to gain an insight into WGS and RWGS reactions in the future.

Acknowledgements

This work was supported by the National Natural Science Foundation of China (grant no. 20273034), the Foundation of State Key Laboratory of Coal Conversion and C1 Chemistry & Technology (Taiyuan University of Technology) of China.

Appendix A

Here are the formulae to calculate the adsorption energies of HCOO (listed in Table 4), activation barriers of forward reactions (ΔE_f) and reversed reactions (E_r) and enthalpy changes (ΔH) for RWGS reaction on the Cu(*hkl*) surfaces (listed in Table 5). For the derivation of these equations, the reader could refer to Refs. [23,24].

A.1. Adsorption energy of HCOO

$$E_{HCOO} = 1.5E_O^2/(E_O + D) \tag{A.1}$$

where E_{HCOO} and E_O denote the adsorption energy of HCOO and oxygen atom, respectively, and $D = 7.2$ eV.

A.2. Activation barriers for dissociation $AB_{s,g} \rightarrow A_s + B_s$

(A) From the gas phase

$$\Delta E_{AB,g} = \frac{1}{2}\{\Delta H + [E_A E_B/(E_A + E_B)]\} \tag{A.2}$$

where $\Delta H = D - (E_{AB} + E_A + E_B)$ and $D = D_{AB} - D_A - D_B$.

(B) From an adsorbed state

$$\Delta E_{AB,s} = \frac{1}{2}\{\Delta H + [E_A E_B/(E_A + E_B)]\} \tag{A.3}$$

where $\Delta H = D + E_{AB} - E_A - E_B$ and $D = D_{AB} - D_A - D_B$.

A.3. Activation barriers for recombination reaction $A_s + B_s \rightarrow AB_{s,g}$

(A) If $\Delta E_{AB,\mathrm{g}} > 0$, then

$$\Delta E_{A-B,\mathrm{s}} = \Delta E_{A-B,\mathrm{g}} = E_A + E_B - D_{AB} + \Delta E_{AB,\mathrm{g}} \quad (A.4)$$

(B) If $\Delta E_{AB,\mathrm{g}} < 0$, then

$$\Delta E_{A-B,\mathrm{g}} = \Delta E_{A-B,\mathrm{s}} - \Delta E_{AB,\mathrm{g}} = E_A + E_B - D_{AB} \quad (A.5)$$

A.4. Activation barriers for a disproportionation reaction $A_s + BC_s \rightarrow AB_s + C_s$

$$\Delta E_{\mathrm{f}} = \frac{1}{2}\{\Delta H + [E_{AB}E_C/(E_{AB} + E_C)]\} \quad (A.6)$$

where $\Delta H = D + E_A + E_{BC} - E_{AB} - E_C$ and $D = D_A + D_{BC} - D_{AB} - D_C$.

A.5. Activation barriers for $CO_{2,\mathrm{g}} \rightarrow CO_{\mathrm{s}} + O_{\mathrm{s}}$ *reaction*

$$\Delta E_{\mathrm{f}} = \Delta E^{*,LJ}_{AB,\mathrm{g}} = \Delta H + [E_A E_B/(E_A + E_B)] \quad (A.7)$$

where $\Delta H = D_{\mathrm{CO\text{–}O}} - (E_A + E_B)$ and $D_{\mathrm{CO\text{–}O}} = 5.52$ eV.

$$\Delta E_{\mathrm{r}} = \Delta E^{*,LJ}_{A-B,\mathrm{g}} = E_A E_B/(E_A + E_B) \quad (A.8)$$

The $CO_{2,\mathrm{g}} \rightarrow CO_{\mathrm{s}} + O_{\mathrm{s}}$ reaction is a special case, and the reader could refer to Ref. [23, pp. 131–132], for a detailed discussion.

References

[1] D.S. Newsome, Catal. Rev. Sci. Eng. 21 (1980) 275.
[2] G.D. Weatherbee, C.H. Bartholomew, J. Catal. 68 (1981) 67.
[3] G.D. Weatherbee, C.H. Bartholomew, J. Catal. 77 (1982) 460.
[4] C.K. Vance, C.H. Bartholomew, Appl. Catal. 7 (1983) 169.
[5] G.D. Weatherbee, C.H. Bartholomew, J. Catal. 87 (1984) 352.
[6] T. van Herwijnen, W.A. de Jong, J. Catal. 63 (1980) 83.
[7] D.C. Grenoble, M.M. Estadt, D.F. Ollis, J. Catal. 67 (1981) 90.
[8] T. Salmi, R. Hakkarainer, Appl. Catal. 49 (1989) 285.
[9] K. Klier, C.W. Young, J.G. Nunan, Ind. Eng. Chem. Fundam. 25 (1986) 36.
[10] E. Fiolitakis, H. Hofman, J. Catal. 80 (1983) 328.
[11] R.A. Handden, H.D. Vandervell, K.C. Waugh, G. Webb, in: Pro. 9th Int. Congr. Catal., Chemical Institute of Canada, Ottawa, Canada, vol. 4, 1988, p. 1853.
[12] K.C. Waugh, Catal. Today 51 (1999) 161.
[13] C.T. Campbell, K.A. Daube, J. Catal. 104 (1987) 108.
[14] J. Nakumura, J.M. Campbell, C.T. Campbell, J. Chem. Soc. Faraday Trans. 86 (1990) 2725.
[15] J. Nakumura, J.A. Rodriguez, C.T. Campbell, J. Phys. (Condens. Mat.) 1 (1989) 149.
[16] K.H. Ernst, C.T. Campbell, G. Moretti, J. Catal. 134 (1992) 66.
[17] J. Yoshihara, C.T. Campbell, J. Catal. 161 (1996) 776.
[18] A.J. Elliott, R.A. Hadden, J. Tabatabaei, K.C. Waugh, F.W. Zemicael, J. Catal. 157 (1995) 153.
[19] I. Fishtik, R. Datta, Surf. Sci. 512 (2002) 229.
[20] G.C. Wang, L. Jiang, Z.S. Cai, Y.M. Pan, N.J. Guan, Y. Wu, X.Z. Zhao, Y.W. Li, Y.H. Sun, B. Zhong, J. Mol. Struct. (Theochem.) 589–590 (2002) 371.
[21] G.C. Wang, L. Jiang, Z.S. Cai, Y.M. Pan, X.Z. Zhao, W. Huang, K.C. Xie, W. Li, Y.H. Sun, B. Zhong, J. Phys. Chem. B 107 (2003) 557.
[22] E. Shustorovich, R.C. Baetzold, Science 227 (1985) 876.
[23] E. Shustorovich, Adv. Catal. 37 (1990) 101.
[24] E. Shustorovich, H. Sellers, Surf. Sci. Rep. 31 (1998) 1.
[25] E. Shustorovich, A.T. Bell, Surf. Sci. 253 (1991) 386.
[26] C.T. Au, C.F. Ng, M.S. Liao, J. Catal. 185 (1999) 12.
[27] K. Hermann, M. Witko, L.G.M. Pettersson, P. Siegbahn, J. Chem. Phys. 99 (1993) 610.
[28] M.A. van Daelen, Y.S. Li, J.M. Newsam, R.A. van Santen, J. Phys. Chem. 100 (1996) 2279.
[29] Z.M. Hu, R.J. Boyd, J. Chem. Phys. 112 (2000) 9562.
[30] R.A. van Santen, M. Neurock, Catal. Rev. Sci. Eng. 37 (1995) 557.
[31] D.R. Lide, CRC Handbook of Chemistry Physics, 79th ed., CRC Press, Boca Raton, FL, 1998.
[32] C.T. Au, M.D. Chen, Chem. Phys. Lett. 278 (1997) 238.
[33] D.A. King, D.P. Woodruff, The Chemical Physics of Solid Surfaces, vol. 7, Phase Transitions Adsorbate Reconstructuring at Metal Surfaces, Elsevier, Amsterdam, 1994.
[34] A.D. Becke, J. Chem. Phys. 98 (1993) 5648.
[35] C. Lee, W. Yang, R.G. Parr, Phys. Rev. B 37 (1988) 785.
[36] M.J. Frisch, et al., Gaussian 94, Revision E.3, Inc., Pittsburgh PA, 1995.
[37] P.J. Hay, W.R. Wadt, J. Chem. Phys. 82 (1985) 299.
[38] F. Solymosi, J. Mol. Catal. 65 (1991) 337.
[39] H.-J. Freund, M.W. Roberts, Surf. Sci. Rep. 25 (1996) 225.
[40] R.A. Hadden, H.D. Vandervell, K.C. Waugh, G. Webb, Catal. Lett. 1 (1988) 27.
[41] R.G. Copperthwaite, P.R. Davies, M.A. Morris, M.W. Roberts, R.A. Ryder, Catal. Lett. 1 (1988) 11.
[42] P.B. Rasmussen, P.A. Taylor, I. Chorkendorff, Surf. Sci. 269–270 (1992) 352.
[43] J. Pritchard, F.C. Tompkins, Trans. Faraday Soc. 56 (1960) 540.

[44] A.G. Goyden, Dissociation Energies Spectra of Diatomic Molecules, Chapman & Hall, London, 1968.
[45] F. Besenbacher, J.K. Nørskov, Prog. Surf. Sci. 44 (1993) 5.
[46] E. Giamello, B. Fubini, P. Lauro, A. Bossi, J. Catal. 87 (1984) 443.
[47] A.C. Pavão, T.C.F. Guimarães, S.K. Lie, C.A. Taft, W.A. Lester Jr., J. Mol. Struct. (Theochem.) 458 (1999) 99.
[48] A. Föhlisch, M. Nyberg, P. Bennich, L. Triguero, J. Hasselström, O. Karis, L.G.M. Pettersson, A. Nilsson, J. Chem. Phys. 112 (2000) 1946.
[49] W.V. Glassey, R. Hoffmann, J. Phys. Chem. B 105 (2001) 3245.
[50] L. Jiang, G.C. Wang, N.J. Guan, et al., Acta Phys. Chim. Sin. (Chinese) 19 (2003) 393.
[51] G. Doyen, G. Ertl, Surf. Sci. 43 (1974) 197.
[52] J.E. Müller, J. Harris, Phys. Rev. Lett. 53 (1984) 2493.
[53] M.W. Ribarsky, W.D. Luedtke, U. Landman, Phys. Rev. B 32 (1985) 1430.
[54] P.A. Thiel, T.E. Madey, Surf. Sci. Rep. 7 (1987) 211.
[55] M.A. Henderson, Surf. Sci. Rep. 46 (1998) 1.
[56] J.M. Campbell, M.E. Domagala, C.T. Campbell, J. Vac. Sci. Technol. A 9 (1991) 1693.
[57] H. Nakano, I. Nakamura, T. Fujitani, J. Nakamura, J. Phys. Chem. B 105 (2001) 1355.
[58] P.A. Taylor, P.B. Rasmussen, C.V. Ovesen, P. Stoltze, I. Chorkendorff, Surf. Sci. 261 (1992) 191.
[59] M. Bowker, R.J. Madix, Surf. Sci. 102 (1981) 542.
[60] D.H.S. Ying, R.J. Madix, J. Catal. 61 (1980) 48.
[61] R.J. Madix, S.G. Telford, Surf. Sci. 277 (1992) 246.
[62] B.A. Sexton, Surf. Sci. 88 (1979) 319.
[63] L.H. Dubois, T.H. Ellis, B.R. Zegarski, S.D. Kevan, Surf. Sci. 172 (1986) 385.
[64] T. Yatsu, H. Nishimura, T. Fujitani, J. Nakamura, J. Catal. 191 (2000) 423.
[65] N.R. Avery, Appl. Surf. Sci. 11/12 (1981) 774.